ON SEISMIC DESIGN OF ECCENTRICALLY BRACED STEEL FRAMES

Kazuhiko Kasai (I)
Egor P. Popov (II)
Presenting Author: Kazuhiko Kasai

SUMMARY

This paper describes the basic characteristics and the available design methods for eccentrically braced frames (EBFs). It is shown that the selected bracing scheme and the ratios of brace eccentricity lengths to beam span lengths play dominant roles on the elastic and plastic behavior of EBFs. A new general method for a rapid preliminary plastic design of EBFs is described and its accuracy is demonstrated by comparisons with elasto-plastic solutions. A summary of the current research being conducted at the University of California at Berkeley is also given.

INTRODUCTION

Since publication of a research paper on EBFs for seismic bracing in 1978 (Ref. 1), this concept has been rapidly adopted in practice. Several major buildings in California have already been constructed using this approach, and others are under construction or are being designed employing this system of bracing. Fig. 1 illustrates several possible types of EBFs: the D-brace, K-brace, and V-brace frames. In all such frames the axial forces in the braces are transmitted to the columns through bending and shear action by a portion of the beam called an "active link." If designed correctly, EBFs possess greater ductility and are more versatile than the concentrically braced frames (CBFs). Moreover, for drift control they offer significant advantages of economy in comparison with moment-resisting frames (MRFs).

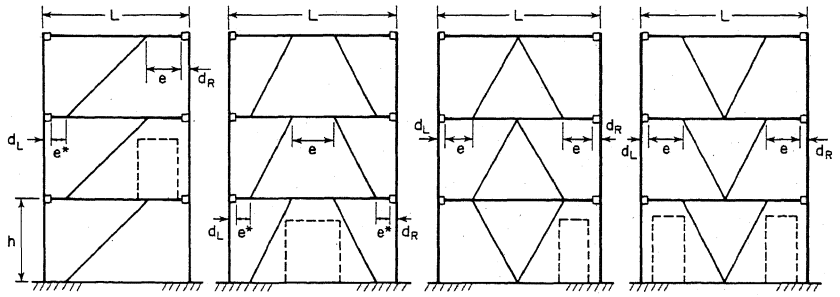

FIG. 1 Various Types of EBFs

(I) Research Assistant, Department of Civil Engineering, University of California, Berkeley, California 94720, USA.

(II) Professor Emeritus of Civil Engineering, University of California, Berkeley, California 94720, USA.

Inelastic Behavior of Shear Links. The performance of an EBF depends largely on the active links. As shown in Fig. 2, for a well-designed structure the inelastic activity is widely distributed so that a large portion of the energy generated by an earthquake can be dissipated. Based on recent analytical and experimental studies at Berkeley, the classification of links given earlier in Ref. 2 is somewhat modified. It is convenient to identify three types of hinges shown in Fig. 2:

1. Plastic hinges of moment M_p [Hinges (1)].
2. Plastic hinges of moment larger than M_p^* and less than M_p which are also subjected to relatively high shear [Hinges (2)].
3. Plastic hinges with moments equal to or less than M_p^* accompanied by web yielding in shear of V_p^* [Hinges (3)].

The basic quantities M_p, M_p^*, and V_p^* associated with the above hinges are defined as follows:

$$M_p = \sigma_y Z \; ; \quad M_p^* = \sigma_y (d - t_f)(b_f - t_w)t_f \; ; \quad V_p^* = (\sigma_y/\sqrt{3})(d - t_f)t_w \quad , \tag{1}$$

where σ_y, Z, d, t_f, b_f, and t_w are the yield stress, plastic modulus, height, flange thickness, flange width, and web thickness of the beam section, respectively. Figure 3 shows a typical M-V interaction curve for the wide flange beam section. The curves can be approximated by Neal's expression as follows (Refs. 3, 4):

$$\frac{(M - M_p^*)^2}{(M_p - M_p^*)^2} + \frac{V^2}{V_p^{*2}} = 1 \quad (M \geq M_p^*) \; ; \qquad V \simeq V_p^* \quad (M < M_p^*) \quad . \tag{2}$$

The maximum shear hinge length b* can be expressed as:

$$b^* = 2M_p^*/V_p^* \quad . \tag{3}$$

The length e for an active link should be less than or equal to b* to ensure that the web yields in shear. Such a link will be called a "shear link." This type of link appears to offer excellent ductility under cyclic loadings if appropriately sized and spaced web stiffeners are provided to prevent web buckling (Refs. 4,5). A link longer than b* is called a "moment link."

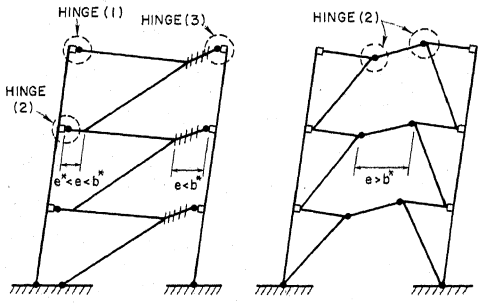

FIG. 2 Collapse Mechanisms of EBFs

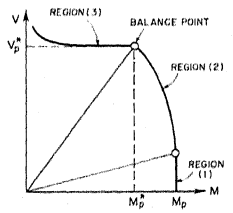

FIG. 3 M-V Interaction Curve for Wide Flange Beams

Collapse Mechanism and Ductility Demand. Fig. 4 shows an appropriate collapse mechanism of a D-brace frame. Subject to kinematic constraints, some latitude in selecting the collapse mechanism is possible. For this selected mechanism to occur, the columns should remain elastic, except for plastic hinges at the base; accordingly, the following recurrence formulas for rigid-plastic displacement fields may be obtained for the ith floor level:

$$\begin{aligned}
\theta_{D(i)} &= [(e^*)^{i-1}/(L - e - e^* - d_L - d_R)^i]\ (e^* + d_L)\theta \simeq 0 \\
\theta_{A(i)} &= L\theta/e - e^*\theta_{D(i-1)}/e \simeq L\theta/e \quad (\theta_{D(0)}: \text{use above eq.}) \\
\theta_{B(i)} &= \theta_{A(i)} - \theta_{D(i)} \simeq L\theta/e \\
\Delta_{B(i)} &= (L - e - d_R)\theta + e^*\theta_{D(i)} \simeq (L - e - d_R)\theta
\end{aligned} \tag{4}$$

The approximate equations are in good agreement with exact solutions for multistory frames; therefore, for purposes of design, Eqs. (4) can be used to estimate the relationships between local member ductility and lateral structure plastic displacement, which can be defined as a displacement after yielding by applying the bilinear approximation on the global structure displacement field. The ductility demand to the active link can be reduced by making the value of e as large as possible.

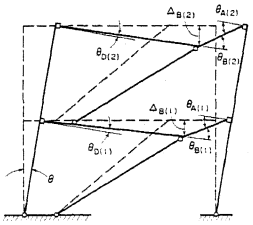

FIG. 4 Rigid Displacement Field of an EBF

The same equations can be used for the K-brace or V-brace frames, making use of geometrical similarity, since they basically have geometry similar to the D-brace. It is then to be noted that, in V-brace frames, if two links of length e equal to that in a D-brace frame are used, the link ductility demand is one-half that for a D-brace frame, provided that the span length L is the same for both frames. The link ductility demand for the K-brace frames is the same as that for the D-brace frames.

Plastic Capacity of EBFs. The discussion above forms a basis for predicting plastic capacity of EBFs. Based on the study in Ref. 6, the upper bound estimate of a collapse load for a frame with shear links can be easily made. For a given virtual displacement θ, the internal work W_I and the external work W_E for the frame of the type shown in Fig. 4 can be expressed as:

$$W_I = \sum_{i=1}^{N} [V^*_{p(i)} e_{(i)} (\theta_{A(i)} + \theta_{B(i)})/2 + M_{D(i)}\theta_{D(i)}] \simeq \sum_{i=1}^{N} V^*_{p(i)} L\theta \tag{5a}$$

$$W_E = \mu \sum_{i=1}^{N} [P_{(i)} h_{(i)} \theta] , \tag{5b}$$

where $P_{(i)}$ and $h_{(i)}$ are, respectively, the generalized lateral load and distance from the ground in the corresponding floor level i in an N-story EBF. The first set of expressions in W_I can be approximated using Eqs. (4), result-

ing in the simplified second expression. In obtaining the latter useful expression, it should be noted that the neglected second term is very small compared to the first, implying that the active hinges absorb most of the energy in an EBF system. By the same token, if columns are fixed at the ground, the energy absorbed by the hinge at the base can usually be neglected, still yielding a good approximation of W_I.

On equating W_I and W_E, one obtains a collapse load factor μ. If vertical loadings are applied to the beams, different collapse mechanism may occur, especially when e* is not zero. (The authors are grateful to Professor H. Gesund for suggesting to emphasize this possibility.) Fig. 5(a) shows the mechanisms of the frame subjected to both lateral and vertical loading equivalent to 0.06 k/in; these mechanisms were obtained with the aid of elasto-plastic large displacement analysis using a newly developed shear beam element (Ref. 7). The beam section used was W14 × 53 and σ_y was assumed to be 36 ksi. The columns and braces were selected such that they remained elastic. The proportions of the frames are the same as the D-brace frame shown in Fig. 8, except that e* = 0 for the frame in Fig. 5(b).

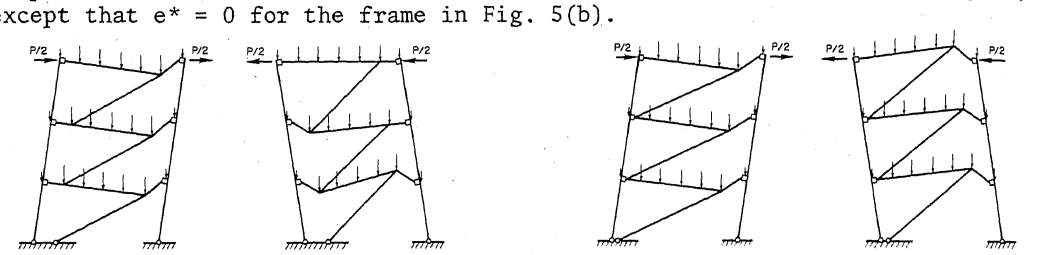

FIG. 5 Mechanism of EBFs due to Lateral and Vertical Loads

In these figures, P_{ult} indicates the magnitude of P obtained at 2% average structure drift in elasto-plastic analysis. It should be noted that for the frame in Fig. 5(a), the location of the active hinges varies depending on the direction of the lateral load when vertical loadings are present, which requires reconsideration of ductility demand on the links. Sometimes this may not be economical, since one has to place web stiffeners on the links of length e*. On the other hand, the frame in Fig. 5(b) shows the fully cyclic inelastic action of the active link can be expected. The same results were obtained for K-brace frames, whereas the V-brace frames showed only one kind of mechanism. Further analyses were done increasing the magnitude of the vertical load by three, and the same mechanisms were found.

Another important aspect of plastic capacity of EBFs can be explained with the aid of Fig. 6. For an assumed typical ratio of Mp* to Mp, the plastic capacity of an EBF can be obtained for the given e/L ratio using Eqs.(2) and (5). The plateau in the figure indicates the range of e/L where shear yielding of the link occurs. It can be seen that the shear link gives a much larger capacity than does the moment link. In extreme case, depending on the span length, the shear link in an EBF can provide 4.5 to 9 times the lateral load resisting capacity of an MRF

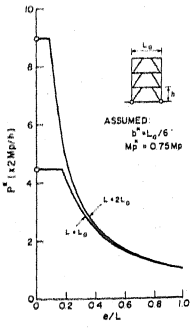

FIG. 6 Capacity of two EBFs vs. e/L

, for which P* = 2Mp/h. Further, the capacity of an EBF with a shear link is proportional to the span length, which follows from Eq. (5), whereas the capacities of EBFs with moment links are almost the same regardless of the span length, when the ductility demand on the links is the same.

PLASTIC DESIGN OF EBFs

Background. The design methods for EBFs were previously presented by Roeder (Ref. 8), Manheim (Ref. 9), and Teal (Ref.10). The first two methods are plastic design methods based on the lower and upper bound theorems for inelastic structures, whereas the latter method is an allowable stress design method utilizing modified safety factors based on code provisions. However, as explained in Ref. 11, these methods seem to present problems of ease of application, accuracy, or consistency; therefore an alternative approach was developed.

Formulation of Solution. Fig. 7 shows a free-body diagram of a D-brace frame at a typical story level, which is subjected to lateral loads P_L and P_R. The magnitudes of the forces transferred from the top of the frame, H_1', H_2', M_1', M_2', P_1', P_2', and B_V', are known from analysis of the floor above. At the top floor level, these quantities are zero. The task is to find both statically and kinematically admissible solutions of the frame. Fortunately, as noted earlier, a unique collapse mechanism can be selected for any given structure, meaning that one can assign plastic hinges deterministically on the frame.

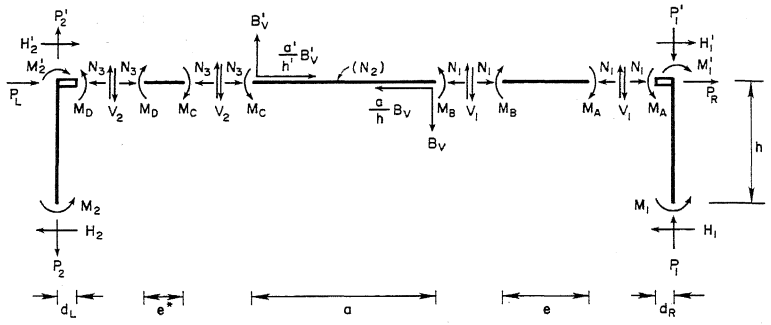

FIG. 7 Free Body Diagram for Design Method

To reduce the static indeterminacy of the system, it is necessary to assume the location of inflection points on the columns, which can be located by a parameter α, the ratio of the bottom to the top column end moments. Further, the following three equations should be considered:

$$M_A = \beta_A(eV_1/2) \quad ; \quad M_B = (2 - \beta_A)(eV_1/2) \; ; \quad M_D = \beta_D(eV_1/2) \; . \tag{6}$$

By assigning the values α, β_A, and β_D, one could solve for a statically admissible field; therefore, an appropriate selection of these parameters is important. It has been found that the values of α vary between 1 and 1.3 when the lateral loading on the structure varies smoothly from story to story. (For a concentrated load at the top, a different assumption must be made.) Also, it is necessary to take

$$\beta_A = b^*/e \geq 1 \ , \tag{7}$$

meaning that the moment of M_p^* develops at points such as A in Fig. 7. It should be noted that this assumption implies unequal end moments in the links, i.e., M_B is less than or at most equal to M_A. In general, the inequality indicated in Eq. (7) applies in order to assure shear link behavior.

β_D can be assumed to be the same as β_A in Eq. (7) if e* is the same as e. However, as stated earlier, it is possible to set e* much smaller than e for a more economical and efficient design. In such a case, β_D can be assumed to be a fraction of β_A. Based on some numerical experimentation, the following equation was found to be useful:

$$\beta_D = [0.2 + 0.8(e^*/e)]\beta_A \ . \tag{8}$$

Assigning the above parameters in the above manner, one can obtain all member forces starting from the top. For a better estimate of β_A given by Eq. (7), an iteration can be performed using the actual b* value of the selected beam, which was found to be very stable. Due to the simplicity of the above procedure, a computer design program based on this method was developed (Ref. 11).

Design Example. The frame types appearing as the first and fourth illustrations in Fig. 1 were used to test the design method. Lateral loads of 200 kips were applied to the top of each frame. The proportions, as well as member sections for the two frames selected by the computer program, are shown in Fig. 8.

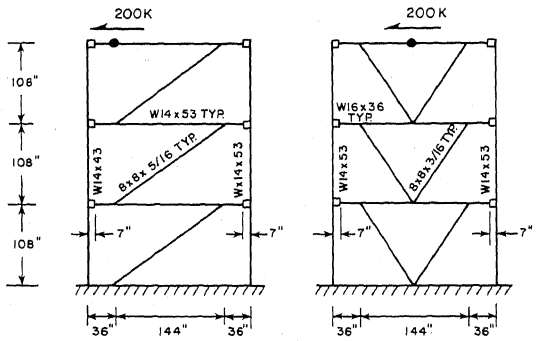

FIG. 8 Proportions and Member Sections for EBFs

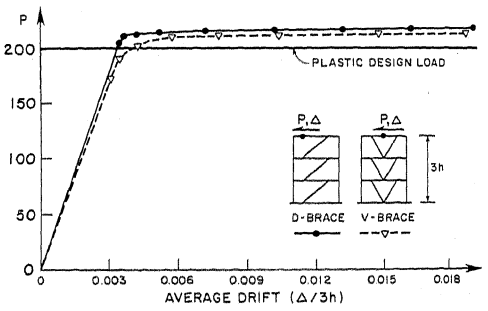

FIG. 9 Load-Deflection Behavior of Designed EBFs

It can be seen from Fig. 9 that the designed frame attained expected capacity. Somewhat earlier yielding of the V-brace links had occurred because lighter sections were selected for the beams than for the D-brace frame. However, the plastic shear deformations of the links at a considerable story drift were about half those in the D-brace frame, as indicated earlier in this paper. The comparison between the moments predicted by the proposed method and elasto-plastic analysis is shown in Figs. 10(a) and 10(b). Some discrepancies, which are not significant from the design viewpoint, occur because the capacities of the selected beams somewhat exceed the design forces. The excess beam capacity was larger in D-brace than in V-brace frames. For the latter frame, the initial design moments in the beams are in excellent agreement with

the results of an elasto-plastic analysis, leading to the conclusion that the proposed design method is exceptionally accurate.

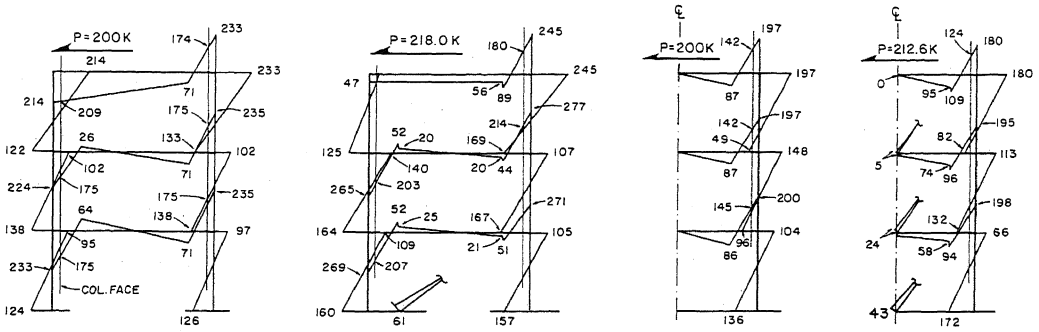

(a) D-brace frame (b) V-brace frame

FIG. 10 Comparison of Design and Analysis Moments

ELASTIC CHARACTERISTICS OF EBFs

One of the unique features of an EBF is that the elastic story stiffness can be controlled by varying the e-value at each story while maintaining its capacity. Research was carried out to determine what range of stiffness is available for this purpose. First, as shown in Fig. 11, the 20-story EBFs employing three types of bracing schemes were plastically designed using the computer program developed. The proportion and design lateral force for those EBFs were in the practical range and similar to those used in Ref. 8. Corresponding to the various values of e, four one-story panels with simulated boundary conditions were analyzed at different floor levels.

Fig. 12 exhibits analytical results for elastic story shear drift of the panels located from these analyses at the 3rd and the 19th floor levels subjected to correcponding plastic design loads. The horizontal axis in this figure indicates the eccentricity ratios, which are e/L for the D-brace and K-brace frames, and 2e/L for the V-brace frame, since a comparison under the same ductility demand on the links is intended. For modeling, shear deformation of the beam was considered and a rigid end zone was assumed based on heights of the beam and column sections.

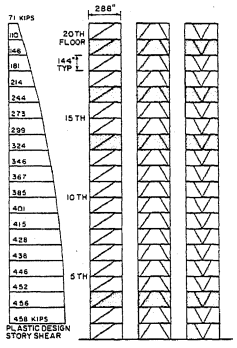

FIG. 11 Plastic Design of 20 story EBFs

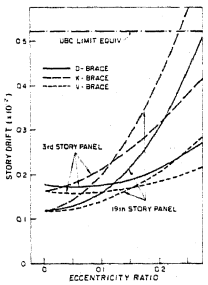

FIG. 12 Dependence of Elastic Shear Drift on Basic Parameters

From this figure, it should be noted that designed EBFs easily satisfy UBC story drift limits (Ref. 12). Also, the maximum stiffness in some case can be attained with no-zero eccentricity. The important point to

observe is that the stiffness of the V-brace frame is much greater than that of the others when the eccentricity ratio is larger than 0.1. The K-brace appears to be the most flexible of all. The decrease of stiffness for increasing the eccentricity ratio is more pronounced for the 19th floor level panels. For further details, see Ref. 11.

CONCLUDING REMARKS

The design and analysis of EBFs discussed above was limited to static loadings. Further work remains to establish rapid methods for dynamic analyses. The development of a computationally efficient shear link element is particularly necessary. Cyclic strain hardening behavior of the link must be included in the algorithm to correspond more accurately with experimental results. The influence of the floor slab and the effect of the axial force on the cyclic behavior of links need further attention. This work currently is being pursued at Berkeley.

ACKNOWLEDGEMENTS

The study reported herein was supported by the National Foundation under Grant No. CEE 81-07217. This support is greatly acknowledged. The help of Gail Feazell in preparing the figures, and of Cindy Polansky in typing the manuscript is greatly appreciated.

REFERENCES

(1) Roeder, C. W. and Popov, E. P., J. Structural Division, ASCE, Vol. 104, No. ST3, March 1978, pp. 391-412.
(2) Popov, E. P. and Malley, J. O., Chapter 11, ASCE Manual on Beam-to-Column Building Connections, in review.
(3) Neal, B. G., J. Mech. and. Engrg. Sci. 3, No. 3, 258 (1961).
(4) Hjelmstad, K. D. and Popov, E. P., J. Structural Engineering, ASCE, Vol. 109, No. ST10, October, pp. 2387-2403.
(5) Malley, J. O. and Popov, E. P., J. Structural Engineering, ASCE, in review.
(6) Manheim, D. N. and Popov, E. P., J. Structural Engineering, ASCE, Vol. 109, No. ST10, October, pp. 2404-2419.
(7) Hjelmstad, K. D. and Popov, E. P., EERC Report 83-15, Earthquake Engineering Research Center, University of California, Berkeley (July 1983).
(8) Roeder, C. W. and Popov, E. P., EERC Report 77-18, Earthquake Engineering Research Center, University of California, Berkeley (Aug. 1977).
(9) Manheim, D. N., D. Eng. thesis, University of California, Berkeley (Feb. 1982).
(10) Teal, E., Structural Steel Educational Council, California Field Ironworkers Administrative Trust.
(11) Kasai, K. and Popov, E. P., EERC Report 83, Earthquake Engineering Research Center, University of California, Berkeley, in preparation.
(12) Uniform Building Code, International Conference of Building Officials, Whittier, California (1982).